agronomy

MDPI

Article

Genome-Wide Identification of Petunia *Hsp20* Gene Family and Functional Characterization of MYC2a-Regulated CIV Subfamily in Pollen Development

Xuecong Zhou †, Bingru Zhang †, Yilin Wang, Letian Wang, Jiajun Tang, Bingyan Zhao, Qian Cheng, Juntao Guo, Hang Zhang and Huirong Hu *

National Key Laboratory for Germplasm Innovation & Utilization of Horticultural Crops, College of Horticulture and Forestry Sciences, Huazhong Agricultural University, Wuhan 430070, China; zhouxuecong@webmail.hzau.edu.cn (X.Z.); zhangbr@webmail.hzau.edu.cn (B.Z.); alan15611120215@163.com (Y.W.); 15267981391@163.com (L.W.); tangjiajun@webmail.hzau.edu.cn (J.T.); lumi@webmail.hzau.edu.cn (B.Z.); 17612716005@163.com (Q.C.); gjt@webmail.hzau.edu.cn (J.G.); guapixi9@163.com (H.Z.)

* Correspondence: huhuirong@mail.hzau.edu.cn

† These authors contributed equally to this work.

Abstract

Plant heat shock proteins (Hsps) are from a diverse and ancient protein family, with small Hsps of ~20 kDa molecular weight classified as Hsp20s. As a key transcription factor in the jasmonic acid (JA) pathway, myelocytomatosis protein 2 (MYC2) plays a vital role in stamen development. In this study, we identified six genes with significantly altered expression levels using previous RNA-Seq data from PhMYC2a-overexpressing and methyl jasmonate (MeJA)-treated petunia. Interestingly, five of these are Hsp20 family members (*PhHsp16.0A*, *PhHsp16.1*, *PhHsp16.8*, *PhHsp21.9*, and *PhHsp40.8*). Yeast one-hybrid (Y1H) and dual-luciferase assays demonstrated that PhMYC2a directly binds their promoters, indicating a collective effect. Thus, a genome-wide analysis was conducted and a total of 38 genes encoding Hsp20s were identified in the reference genome of *Petunia axillaris*. Phylogenetic analysis revealed that 38 members of *Hsp20s* were irregularly distributed on 34 chromosome scaffolds and separated into 13 subfamilies, with only PaHsp16.0A and 16.1, among the five selected Hsp20s, being in the same Cytosol IV (CIV) subfamily. Conserved motif analysis suggested that the *PaHsp20* gene family members may have a high degree of conservation. The promoter sequence analysis suggested that the promoter regions of *PaHsp20* genes contained multiple light- and hormone-related cis-regulatory elements. Subsequently, spatiotemporal expression patterns, analyzed by qRT-PCR, showed that *PhHsp16.0A* and *PhHsp16.1* had relatively high expression levels in flowers, with similar expression patterns at various stages of flower bud and anther development. Furthermore, virus-induced gene silencing (VIGS) of *PhHsp16.0A* and *PhHsp16.1* resulted in significantly reduced pollen fertility, indicating their regulation in the process of flower development and echoing the role of PhMYC2a. This study highlights the pivotal role of Hsp20s in MYC2a-mediated regulatory mechanisms during petunia pollen development.

Keywords: petunia; *Hsp20* gene family; pollen development; VIGS; PhMYC2a

check for updates

Academic Editor: Dilip R. Panthee

Received: 16 July 2025
Revised: 21 August 2025
Accepted: 24 August 2025
Published: 26 August 2025

Citation: Zhou, X.; Zhang, B.; Wang, Y.; Wang, L.; Tang, J.; Zhao, B.; Cheng, Q.; Guo, J.; Zhang, H.; Hu, H. Genome-Wide Identification of Petunia *Hsp20* Gene Family and Functional Characterization of MYC2a-Regulated CIV Subfamily in Pollen Development. *Agronomy* **2025**, *15*, 2048. https://doi.org/10.3390/agronomy15092048

Copyright: © 2025 by the authors. Licensee MDPI, Basel, Switzerland. This article is an open access article distributed under the terms and conditions of the Creative Commons Attribution (CC BY) license (https://creativecommons.org/licenses/by/4.0/).

1. Introduction

Stamen is the male reproductive organ of angiosperms, which participates in the reproductive process by producing pollen [1]. Meanwhile, defects in stamen development

will lead to male sterility. Numerous studies have shown that hormones such as JA, gibberellin (GA), auxin (IAA), abscisic acid (ABA), and cytokinin (CTK) mainly regulate stamen growth through complex molecular regulatory networks [2]. In rice, OsTIE1 tightly regulates JA biosynthesis by inhibiting the TCP transcription factors OsTCP1/PCF5, affecting rice anther dehiscence and male fertility [3]. Similarly, AtHMGB15 acts as a positive regulator in the JA signaling pathway and cooperates with MYC2 to regulate the development of plant male organs [4]. In lily anthers, stable GA levels are critical for microspore-to-pollen transition; research found that silencing *LoBLH6* perturbs this stability, causing abnormal pollen development [5]. *OsFTIP7* promotes nuclear localization of the transcription factor OSH1, which directly represses the IAA biosynthesis gene *OsYUCCA4* during late anther development, thereby regulating the timing of anther dehiscence at flowering and affecting stamen fertility in rice [6]. CRISPR/Cas9-mediated knockout of *LOGL8*, a CTK-activating enzyme gene, predominantly impairs pollen fertility in rice [7]. In tomato, overexpression of *SlCIN2* leads to high glucose levels in anthers, which causes accumulation of ABA and reactive oxygen species (ROS). This disrupts the programmed cell death process in anthers, resulting in pollen abortion [8]. Moreover, the influence of hormones on anther development is not singular. GA affects almond anther development by regulating the expression levels of genes related to IAA, CTK, JA, salicylic acid (SA) and ABA hormones, as well as anther developmental genes [9].

Heat shock proteins, acting as molecular chaperones, are highly conserved proteins involved in plant growth and development. Their expression is significantly induced under environmental stress [10]. Functionally, Hsps maintain cellular homeostasis by aiding the correct folding, repair, and degradation of misfolded proteins, thereby alleviating stress-induced damage to organisms [11,12]. Phylogenetically, eukaryotic Hsps are categorized into five major classes based on molecular weight and homology: Hsp100, Hsp90, Hsp70, Hsp60, and the small heat shock protein family Hsp20 [13]. Among these, Hsp20 proteins typically range in size from 12 to 42 kDa [14].

The *Hsp20* family has been extensively studied in several model plants and in a range of important agricultural and horticultural crops, such as *Arabidopsis thaliana* [15], *Oryza sativa* [16], *Capsicum annuum* [17], *Solanum lycopersicum* [18], *Cucumis sativus* [19], and *Rhododendron delavayi* [20]. Functional characterization has shown that Hsp20s are involved not only in stress response but also in the regulation of plant growth and development. For example, the *A. thaliana Hsp20* gene affects early seed development [21]; meanwhile, the wheat chloroplast small heat stress protein sHsp26 is not only involved in seed maturation and germination but also contributes to seed heat tolerance. Additionally, overexpression of the *OsHsp16.9* gene enhances salt and drought resistance in *O. sativa* [22]; the *Vitis vinifera VvHsp20* gene is involved in fruit development [23]; the *MdHsp18.2b* gene in *Malus domestica* regulates resistance to salt stress and infestation by *Bacillus speciosus*, as well as anthocyanin accumulation in healing tissues [24]; and *A. thaliana* strains overexpressing the *Prunus persica PpHsp20-32* gene exhibit significantly greater plant height than the wild type [25]. Members of the *Hsp20* family regulate various biological processes in organisms. However, limited research has focused on *Hsp20s* in ornamental plants, particularly regarding their roles in growth and development.

Petunia hybrida, an herbaceous flower of the Solanaceae family, is widely used in flower beds due to its rich varieties, diverse flower types, and bright colors [26]. *P. hybrida* relies heavily on hybrid breeding for cultivar improvement, and the utilization of male-sterile lines can effectively shorten the breeding cycles and accelerate seed production. Male sterility also offers several advantages: it helps eliminate pollen allergens, avoids pollen-mediated genetic drift in transgenic plants, and prevents fruit contamination. Furthermore, photosynthetic products retained from blocked anther development promote the

enlargement of other floral organs and prolong the flowering period, thereby enhancing the ornamental quality of flowers [27,28]. Therefore, unraveling the molecular network underlying anther development in petunia will lay a solid foundation for future molecular breeding efforts.

MYC2a, as a core transcription factor of the JA pathway, plays an important role in stamen development [29]. Previously, we performed transcriptome sequencing on anther extremely sterile petunia *PhMYC2a*-overexpressing T1 lines and MeJA-treatment plants (accession number: PRJNA1308536), and the *PhHsp20* genes shared between these two groups attracted our attention. We thus hypothesize that *Hsp20* genes may act as targets of the MYC2a transcription factor, participating in the MYC2a-centered regulatory network governing petunia stamen development. In this study, five *Hsp20* genes were identified from six differentially expressed genes (DEGs) through RNA-Seq data mining, with Y1H and dual-luciferase assays validating their roles as downstream targets of the transcription factor PhMYC2a. Additionally, genome-wide characterization of the Hsp20 gene family was performed, covering evolutionary features, structural properties, regulatory elements, and expression patterns. Focusing on members with notable expression in floral tissues, we further investigated the functional relevance of two CIV subfamily genes (*PhHsp16.0A* and *PhHsp16.1*) in pollen development using VIGS. Together, these analyses aim to clarify the regulatory and functional landscape of *Hsp20s* in petunia reproductive development, providing insights into their roles beyond stress responses.

2. Materials and Methods

2.1. Plant Materials

P. hybrida 'W115' (Mitchell), which was grown in the experimental base of Huazhong Agricultural University (Wuhan, China) at 22 °C under a 16 h light (100 μmol m^{-2} s^{-1}) and 8 h dark photoperiod, was used for gene cloning, expression analyses, and VIGS assays. Young leaves were used to extract genomic DNA and cDNA (reverse-transcribed from RNA) for cloning of the promoter region and genes. Flower anthers (a) and buds (b) were sampled at developmental stages of 0.2a (b), 0.3a (b), 0.5a (b), 1.0a (b), 1.5a (b), 2.5a (b), and 3.5a (b). These stages correspond to bud lengths of 0.2, 0.3, 0.5, 1.0, 1.5, 2.5, and 3.5 cm (with a deviation range of ±0.2 mm). In addition, young roots, young stems, young leaves, unopened flowers, and floral organs of opening flowers (consisting of four whorls: sepal, petal, anther, pistil) were separately collected from three individual plants. These samples were used to extract RNA for qRT-PCR analyses. *Nicotiana benthamiana*, which was planted in the same environment as petunia, was used for dual-luciferase assays. All primers used in this study are listed in Table S1.

2.2. Characterization of PaHsp20 Family Members in Petunia

Genomic and proteomic sequence data of *P. axillaris* (the closest relative of *P. hybrida* 'W115') were downloaded from the Sol Genomics Network (SGN, https://www.sgn.cornell.edu/, accessed on 28 February 2024). The Hidden Markov Model (PF00011) of the Hsp20 domain was downloaded from Pfam (http://pfam.xfam.org/, accessed on 28 February 2024), and an HMM search was performed against the *P. axillaris* genomic and proteomic sequences (from SGN) using the HMMER 3.0 software to select candidate proteins with E-value $\leq 1 \times 10^{-5}$. Candidate protein sequences were submitted to the InterPro (https://www.ebi.ac.uk/interpro/search/, accessed on 5 March 2024) for screening and retention of those containing Hsp20 domains, with their domain positions recorded and sequences with molecular weights outside the 12–42 kDa range removed. ExPASy (https://web.expasy.org/protparam/, accessed on 8 March 2024) was then used to predict the physicochemical

properties of the proteins: molecular mass (Mw), isoelectric point (pI), and grand average of hydropathicity (GRAVY).

2.3. Homologous Sequence Alignment and Phylogenetic Analysis

Phylogenetic analysis was performed using Hsp20 protein sequences derived from *A. thaliana* [15], *O. sativa* [16], and *P. axillaris* (Table S2). All Hsp20 protein sequences were aligned using MUSCLE for multiple sequence alignment, and the phylogenetic tree was then constructed using the neighbor-joining (NJ) method in MEGA 11.0 software with bootstrap value set to 1000. The phylogenetic tree was visualized using ChiPlot (https://www.chiplot.online/circleTree.html, accessed on 20 March 2024) [30]. The protein sequences of PaHsp20s were submitted to Plant-mPLoc (http://www.csbio.sjtu.edu.cn/bioinf/plant-multi/, accessed on 25 March 2024) and WoLF PSORT (https://psort.hgc.jp/, accessed on 25 March 2024) for subcellular localization prediction, and consensus results were selected, which provided a reference for subsequent gene classification.

2.4. Conserved Motifs, Gene Structure, and Promoter Cis-Acting Element Analysis

Thirty-eight PaHsp20 protein sequences were submitted to MEME (https://meme-suite.org/meme/index.html, accessed on 2 April 2024) for conserved motif analysis, a total of ten conserved motifs were identified, and the CDS and UTR positions of the sequences were determined using TBtools v2.0 software. Using the above data, 1500 bp upstream of each CDS was selected as the promoter region. These regions were further analyzed using PlantCARE (http://bioinformatics.psb.ugent.be/webtools/plantcare/html/, accessed on 10 April 2024) to identify promoter cis-elements, and the results were visualized [31]. Images of promoter cis-element counts were generated using ChiPlot (accessed on 14 April 2024).

2.5. Gene Expression Analysis

Total RNA was extracted from different samples of *P. hybrida* using an EASYspin Plant RNA Kit (Aidlab, Beijing, China). First-strand cDNA was synthesized using a HiScript® II Q RT SuperMix for qPCR (Vazyme, Nanjing, China) following the manufacturer's protocol. The qRT-PCR was performed using ChamQ Universal SYBR qPCR Master Mix (Vazyme, Nanjing, China) on ABI 7500/7500-Fast Real-Time PCR system (Applied Biosystems, Foster City, CA, USA) according to a previously described method. The $2^{-\Delta\Delta Ct}$ method was used to calculate relative expression levels, which were normalized to the expression of the housekeeping gene EF-1α across different tissues.

2.6. Y1H Assays

The CDS region of *PhMYC2a* was integrated into the *NdeI* and *XhoI* sites of pGADT7 vector via homologous ligation. The pHIS2 vector was cleaved with *Eco*RI and *Sac*I restriction enzymes, and the promoter sequences of *PhHsps* were cloned into it using the same ligation method. The Y1H assay was performed as the previous protocol [32]. Each recombinant pHIS2 construct (containing PhHsps promoters) was cotransformed with pGADT7-PhMYC2a into Y187 yeast cells. The pGADT7 vector was used as a negative control. The binding of PhMYC2a to each promoter fragment was assessed on SD/-Leu/-Trp/-His medium containing 20, 50, 60, or 70 mM 3-amino-1,2,4-triazole (3-AT), which was used to suppress background histidine leakage of the pHIS2 vector.

2.7. Dual-Luciferase Assays

For the effector plasmid, the coding sequence of *PhMYC2a* was cloned into the pGreenII 62-SK vector at the restriction sites *SmaI* and *KpnI* to obtain 35S:*PhMYC2a* as effector construct. The same restriction enzymes were used to cleave the pGreenII 0800-LUC vector,

the promoter sequences of *PhHsps* were cloned into it to form *proPhHsps*:LUC reporters using a ClonExpress II one-step cloning kit. The effector and reporters were transformed into *Agrobacterium tumefaciens* GV3101 (pSoup-19) and then co-expressed in *N. benthamiana* leaves. The empty vector was used as a negative control. After 48 to 60 h of transformation, the luciferase activity was measured with a *TransDetect*® Dual-Luciferase Reporter Gene Assay kit (TransGen, Beijing, China). Three biological replicates were performed to quantify luciferase activity.

2.8. Virus-Induced Gene Silencing in P. hybrida

Specific cDNA fragments (200 bp for *PhHsp16.0A* and 190 bp for *PhHsp16.1*) were amplified and cloned into the pTRV2 vector using the *EcoRI* and *BamHI* sites. VIGS was performed as described [33]. *A. tumefaciens* GV3101 carrying the pTRV1 vector and either pTRV2 (control) or pTRV2-*PhHsp16.0A/16.1* (OD_{600} = 2.0) cultures were mixed in a 1:1 ratio, and the mixture was infiltrated into petunia seedling leaves using a 1 mL sterile needleless syringe.

2.9. Pollen Fertility Test

Viability and in vitro germination assays were employed to verify the pollen fertility, following the method described by Huang et al. [34]. Pollen grains were observed using a bright-field inverted microscope (model TE-2000U, Nikon, Tokyo, Japan) at 10× magnification. Each experiment included three fully bloomed flowers from different VIGS lines and the control group (CK), with three independent biological replicates.

2.10. Statistical Analysis

Statistical analysis was performed using the GraphPad Prism 9 software. Significant analysis of data for rosette area, silique length, and seed length was conducted using Student's *t*-test, with a significance level set at $p < 0.05$.

3. Results and Analysis

3.1. Transcription Factor PhMYC2a Binds Directly to the Promoters of PhHsp20 Genes

To identify the potential downstream targets of PhMYC2a, we analyzed RNA-Seq data from petunia plants with PhMYC2a overexpression and those treated with MeJA. The transcriptomic samples and their conditions are summarized in Table S3. Using DESeq2 software version 1.30.1, we identified differentially expressed genes (DEGs) with the screening criteria of absolute fold change ($|\text{FoldChange}| \geq 3$ and false discovery rate (FDR) ≤ 0.01. A Venn diagram (Figure 1) was constructed to visualize overlapping DEGs across these groups, revealing six DEGs shared between the PhMYC2a-overexpressing and MeJA-treated samples. Detailed functional annotations of these six DEGs are provided in Table 1. Notably, five of these DEGs encode Hsp20 proteins, suggesting that Hsp20s may act as key effectors in the regulatory network mediated by PhMYC2a.

Table 1. Functional annotations of the six shared DEGs.

Name	Gene ID	Functional Annotation
PhHsp21.9	Peaxi162Scf00011g00203	22.7 kDa class IV heat shock protein
PhGOLS10A	Peaxi162Scf00058g02212	Galactinol synthase 1
PhHsp16.8	Peaxi162Scf00128g00741	Small heat shock protein, chloroplastic
PhHsp16.1	Peaxi162Scf00132g00087	17.6 kDa class I heat shock protein
PhHsp16.0A	Peaxi162Scf00420g00141	18.1 kDa class I heat shock protein
PhHsp40.8	Peaxi162Scf00565g00812	17.6 kDa class II heat shock protein

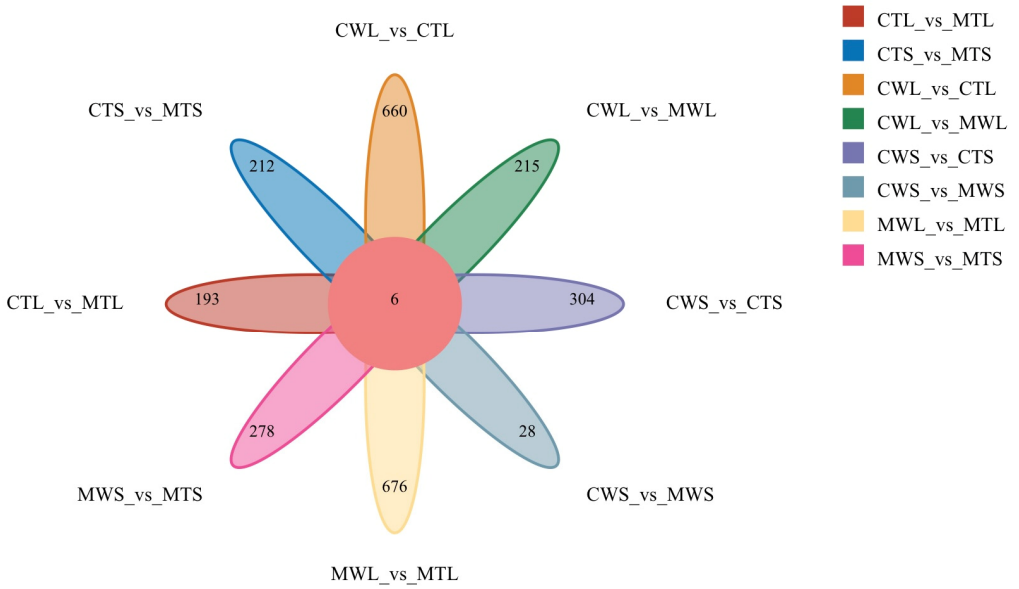


Figure 1. Venn diagram of DEGs in eight different groups. Abbreviations: C (without MeJA treatment) and M (with MeJA treatment); W (non-transgenic plants) and T (transgenic plants); S (small flower size) and L (large flower size).

To verify whether PhMYC2a binds directly to the promoters of these *PhHsp20* genes, we performed a Y1H assay using the *PhHsp20* gene promoters fused to the *HIS3* reporter gene (Figure 2A). As a positive control, yeast cells co-expressing pGADT7-53 and p53HIS2 grew normally on -Leu/-Trp/-His media with any concentration of 3-aminotriazole (3-AT). For our test samples, yeast cells co-expressing *PhMYC2a*-pGADT7 and *proPhHsp16.0A/16.1/16.8/21.9*-pHIS2 grew normally on -Leu/-Trp/-His media with 60, 20, 50, and 20 mM of 3-AT, respectively. In contrast, yeast cells co-expressing an empty pGADT7 vector and the same *proPhHsp*-pHIS2 reporters failed to grow under these conditions (Figure 2B–E). These results indicate that PhMYC2a directly binds to the promoters of *PhHsp16.0A*, *PhHsp16.1*, *PhHsp16.8*, and *PhHsp21.9*. Notably, both yeast cells co-expressing pGADT7 and *proPhHsp40.8*-pHIS2, as well as those co-expressing PhMYC2a-pGADT7 and *proPhHsp40.8*-pHIS2, grew normally on -Leu/-Trp/-His media with 70 mM 3-AT, but the latter was shown to be significantly stronger (Figure 2F), suggesting that PhMYC2a may also bind to the promoter of *PhHsp40.8*.

Having shown PhMYC2a directly binds to the *PhHsp20* promoters via Y1H assays, we further performed dual-luciferase reporter assays to confirm these bindings in a plant cellular context. The effector vector *35S:PhMYC2a* was constructed by fusing *PhMYC2a* to the 35S promoter. Reporter vectors *proPhHsps*:LUC were generated by inserting *PhHsp20* gene promoters upstream of LUC gene (Figure 3A). Dual-luciferase assays showed that the ratio of luciferase to Renilla luciferase (LUC/REN) activity was significantly higher in samples co-expressing *35S:PhMYC2a* and *proPhHsp16.0A/16.1/16.8/21.9/40.8:* LUC compared to controls (empty effector + *proPhHsps:*LUC). Specifically, the LUC/REN ratios were 2.75-, 2.53-, 1.56-, 2.46-, and 1.83-fold higher (Figure 3B). These results confirm that PhMYC2a directly binds to the *PhHsp20* promoters, consistent with the findings from Y1H assays.

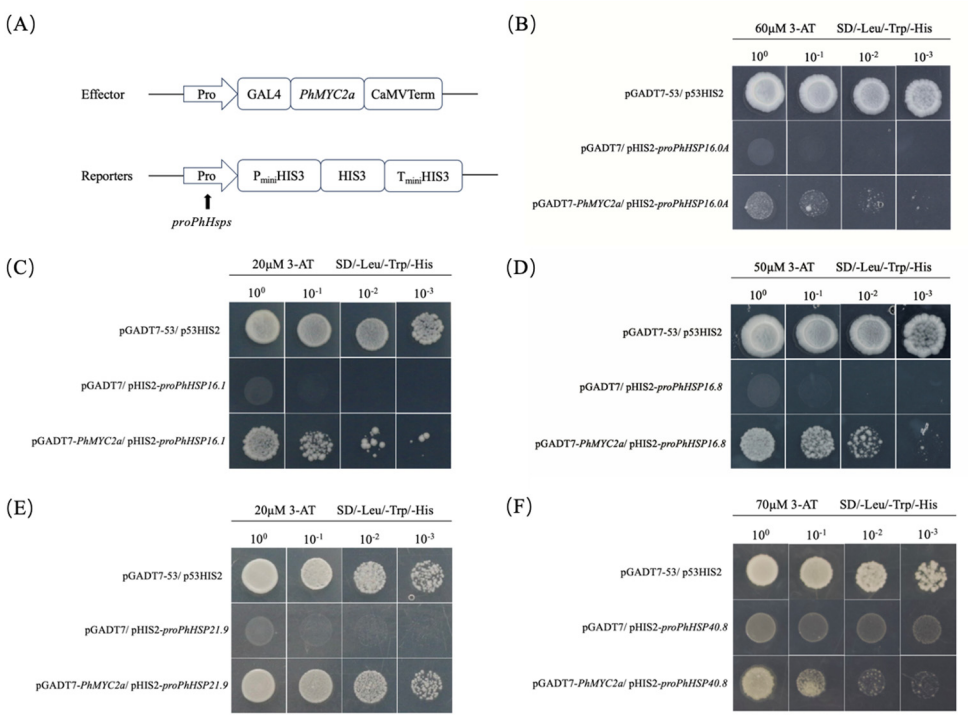


Figure 2. The results of yeast one-hybrid assay. (**A**) Schematic of vectors used in Y1H assays; (**B**) PhMYC2a binds the promoter of *PhHsp16.0A*; (**C**) PhMYC2a binds the promoter of *PhHsp16.1*; (**D**) PhMYC2a binds the promoter of *PhHsp16.8*; (**E**) PhMYC2a binds the promoter of *PhHsp21.9*; (**F**) PhMYC2a may bind the promoter of *PhHsp40.8*.

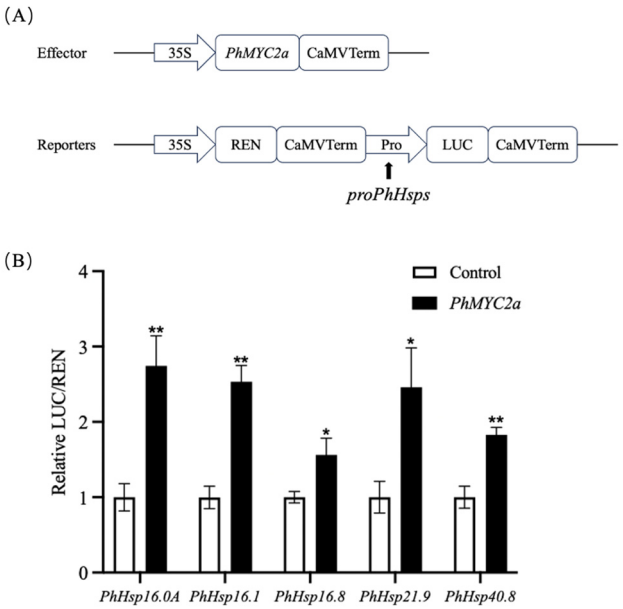


Figure 3. The results of dual-luciferase reporter assays. (**A**) Schematic of the vectors used to perform dual-Luciferase reporter assay; (**B**) LUC/REN activity ratios of dual-luciferase assay, asterisks represent statistically significant differences (* $p < 0.05$ and ** $p < 0.01$) as determined by Student's *t* test.

3.2. Characterization of the PaHsp20 Gene Family in Petunia

To further explore the evolutionary relationships, structural characteristics, and potential roles of Hsp20s in flower development, we performed a genome-wide identification of *Hsp20* genes using the *P. axillaris* genome database as a reference. A total of 38 Petunia *Hsp20* family members with molecular weights between 12 kDa and 42 kDa were screened

by HMM search and the verification of Hsp20 structural domains on the InterProScan website by excluding those that did not contain Hsp20 structural domains. The molecular weight, isoelectric point, and total average hydrophobicity coefficient of the PaHsp20 family proteins were analyzed, the proteins were named according to the molecular weight size of the proteins, and the proteins with the same molecular weight were named as A, B and C, from the smallest to the largest (Table S4). According to the data in Table 1, the length of coding amino acids ranged from 113 to 379 aa, and the molecular weight size ranged from 12.85 kDa to 41.64 kDa. The one with the highest number of amino acids (379) and the largest molecular weight (41.64 kDa) is PaHsp41.6, and the one with the lowest number of amino acids (113) and the smallest molecular weight (12.85 kDa) is PaHsp12.8. 24 of the members have a theoretical isoelectric point of less than 7, which makes the protein acidic, while 15 members have a theoretical isoelectric point of more than 7, which makes the protein basic. The total of 38 members had a total average hydrophobicity coefficient less than 0, and the protein was hydrophilic.

3.3. Chromosomal Localization and Phylogenetic Analysis

The 38 members of the *PaHsp20* family of petunia are distributed on 34 chromosome scaffolds (Figure 4), the chromosomes are populated by gene density, with bluer colors representing fewer gene sequences and redder colors representing denser gene sequences. Meanwhile, it can be found that genes on the same chromosome, such as PaHsp18.0B, PaHsp18.0C, and PaHsp35.7; PaHsp31.8 and PaHsp16.4 are the closest to each other on the branches of the evolutionary tree and belong to the same subfamily, so we speculate that they may have similar functions. However, PaHsp16.1 and PaHsp20.1, which are also on the same chromosome, belong to subfamilies CIV and CIX, respectively.

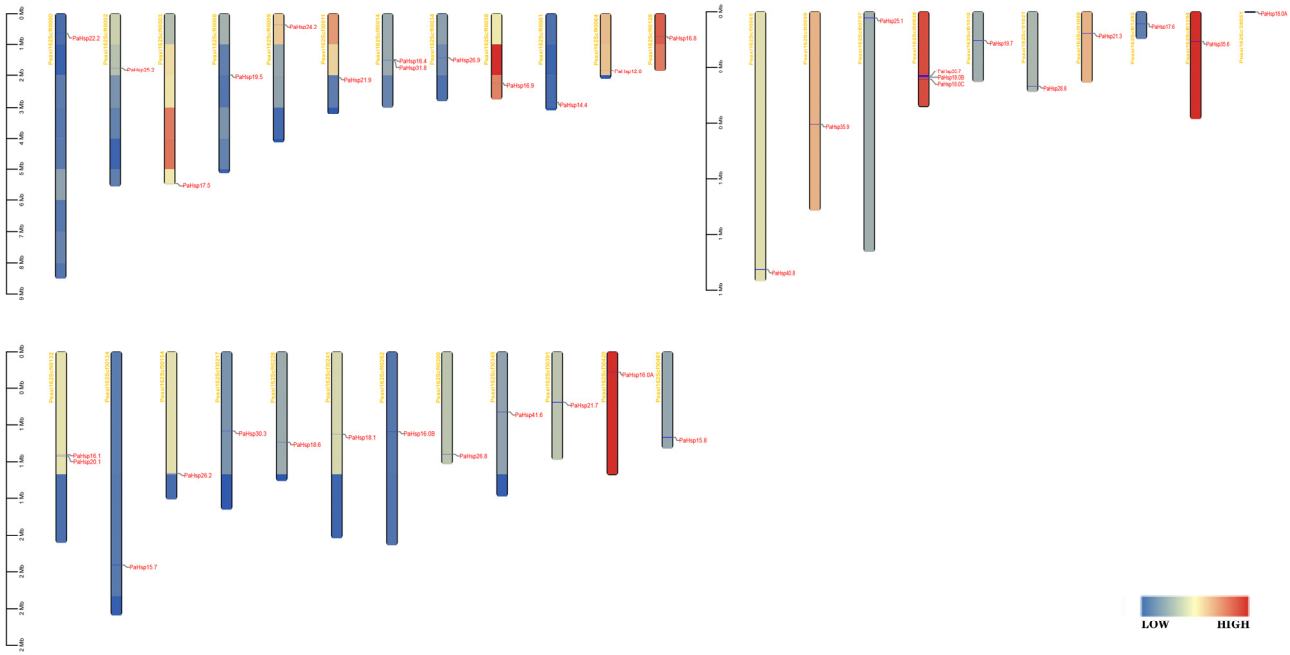


Figure 4. Chromosomal localization of *PaHsp20* gene. The color from blue to red represents a low to high density of genes on that chromosome scaffolding.

A phylogenetic tree was constructed using Hsp20 protein sequences from *O. sativa*, *A. thaliana*, and the above 38 PaHsp20, totaling 79 protein sequences, for sequence alignment (Figure 5). According to the evolutionary branching, the resulting tree revealed that 29 *PsHsp20* genes (76.3%) could be classified into 13 subfamilies based on evolutionary branching and established nomenclature from *A. thaliana* and *O. sativa*, except for the un-

classified *Hsp20*. The largest subgroup, CI, contained eight genes, followed by subfamilies CII, CVIII, CIX, MII, and ER with three genes each. Two genes were assigned to both CIV and CVI, while single-gene representation was observed in CIII, CV, CVII, P, and Px. The remaining nine genes (23.7%) exhibited substantial sequence divergence and could not be assigned to known subfamilies. Among these unclassified members, seven (PaHsp14.4, PaHsp17.5, PaHsp24.2, PaHsp26.2, PaHsp28.8, PaHsp30.3, and PaHsp41.6) formed a distinct cluster designated unknown localization one, while two (PaHsp35.6 and PaHsp35.9) comprised unknown localization two.

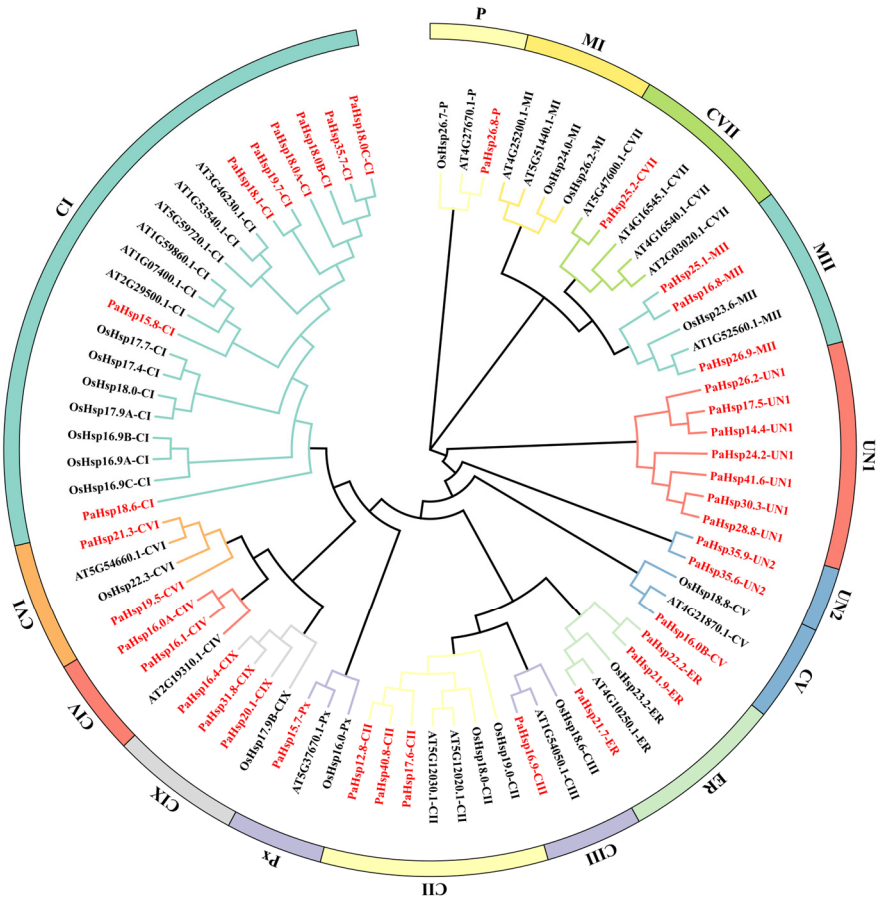


Figure 5. Phylogenetic relationships of Hsp20 in *O. sativa*, *A. thaliana*, and *P. axillaris*. MEGA 11.0 was adopted for phylogenetic analysis by using the Neighbor Joining (NJ) method with 1000 replicates of bootstrapping to test the reliability. The 13 subfamilies were highlighted and differentiated by colors and the unclassified PaHsp20s are represented by the UN1/UN2. Cytosol (C) subfamilies (CI-CIX); mitochondria (M) subfamilies (MI and MII); endoplasmic reticulum (ER), chloroplast (P), and peroxisome (Px).

3.4. Protein Conserved Motifs, Gene Structure, and Promoter Cis-Acting Element Analysis

Ten conserved motifs of PaHsp20 proteins were identified by the MEME website and listed in Table 2, and the lengths of these conserved motifs ranged from 15 to 50 amino acids (Figure 6A, Table 2).

According to the results of the conserved motifs in Figure 6, most PaHsp20 have multiple motifs among these 38 sequences, while PaHsp26.2 has only motif 2; PaHsp25.2 and PaHsp26.8 have only motifs 1 and 2; PaHsp21.3 has only motifs 2 and 5; and PaHsp14.4 and PaHsp17.5 have only motifs 1 and 5. Comparison revealed that the closer the kinship, the closer the number and position of motif distribution of the gene family members, suggesting that the PaHsp20 gene family members may have a high degree of conservatism.

Table 2. List of the putative motifs of PaHsp20 proteins.

Name	Amino Acid Sequence	Sequence Length [1]
Motif 1	LPENAKLDKIKAKMENGVLTV	21
Motif 2	HIFRVDLPGLKKEEVKVZVEE	21
Motif 3	FFGGRRSNIFDPFSLDIFDPFEGFPFSGTVANIPSSARETSAFANARIDW	50
Motif 4	EKNDKWHRMERSSGKFVRRFR	21
Motif 5	GRVLKISGERKREZE	15
Motif 6	PKZEEKKPEVKAIDI	15
Motif 7	SAMAAARVDWKETPEA	16
Motif 8	LAAKLKMPRKVJNMTLVALLVLGIGLYVANVMKS	34
Motif 9	FYNNCVSPSCRNGNNKIKAMAVGERNNLDHLQRQKKHQSNQPRKRSVQMA	50
Motif 10	HGFGGGRGNNVFDPFSLDIWDPFEDFH	27

[1] the length of motif amino acid sequence. Note: A–alanine; C–cysteine; D–aspartic acid; E–glutamic acid; F–phenylalanine; G–glycine; H–histidine; I–isoleucine acid; K–lysine; L–leucine; M–methionine; N–aspartic acid; P–proline; Q–glutamine; R–arginine; S–serine; T–threon amino acid; V–valine; W–tryptophan; Y–tyrosine.

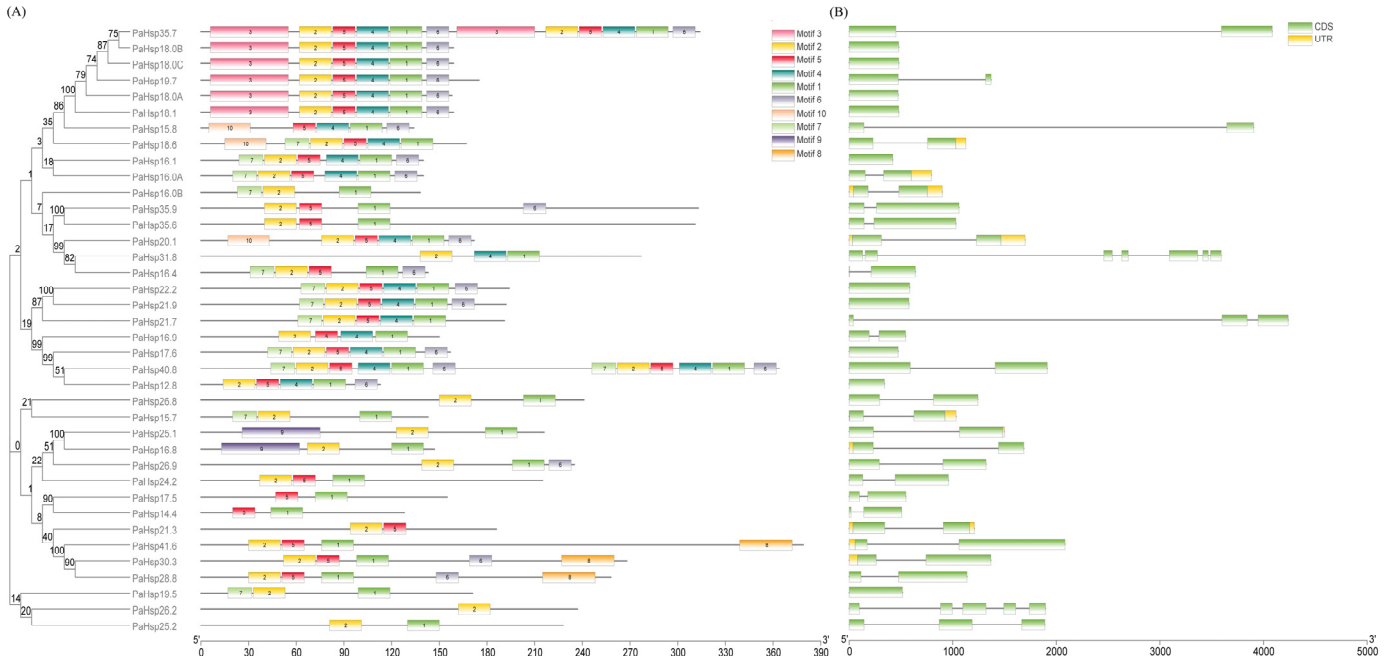


Figure 6. The predicted motifs of PaHsp20 protein and analysis of gene structure of *PaHsp20* family.

The CDS and UTR fragments of the 38 sequences obtained from the analysis (Figure 6B), each of which has two or more CDS fragments. However, *PaHsp16.8*, *PaHsp41.6*, and *PaHsp30.3* had 5′ UTR region; *PaHsp18.6*, *PaHsp16.0A*, *PaHsp15.7*, and *PaHsp25.1* had 3′ UTR region; and *PaHsp16.0B*, *PaHsp20.1*, and *PaHsp21.3* have UTR regions at both 3′ and 5′ ends. Although the UTR acts as an untranslated region and is not a protein coding region, the upstream readable frames within the 5′ UTR region can be translated into polypeptides with transcriptional regulation. A total of 10 (26.3%) *PaHsp20* had no introns, 24 (63.2%) *PaHsp20* had one intron, two (5.3%) *PaHsp20* had two introns, *PaHsp26.2* had four introns, and *PaHsp31.8* had six introns.

In this study, the promoter sequences of 38 *PaHsp20* gene family members were analyzed. The results of promoter cis-acting element analysis showed that the *PaHsp20* family genes have basic core sequences such as TATA-box, CAAT-box, and five of these genes also contain the conserved sequence A-box. All genes except *PaHsp18.0A* have at least one light-responsive element, such as TCT-motif, GT1-motif, GATA-motif, G-box, etc. All genes except *PaHsp30.3* had at least one phytohormone-related response element. For example, 26 genes (68.4%) were related to ABA, 19 genes (50%) were related to GA, 13 (34.2%) genes were related to SA, 23 genes (60.5%) were related to MeJA, and

16 genes (42.1%) were related to IAA. In addition, there were 27, 15, 13, 11, 9, 8, and 7 genes with anaerobic induction element ARE, MYB binding site involved in drought-inducibility MBS, cis-acting element involved in defense and stress responsiveness TC-rich repeats, low temperature response element LTR, cis-acting regulatory element related to meristem expression CAT-box, cis-acting regulatory element involved in circadian control circadian, and cis-acting regulatory element involved in zein metabolism regulation O2-site, respectively. In addition to the above cis-acting elements, the promoters of a small number of genes have regulatory elements related to seed-specific regulation, endosperm expression and specificity, cell cycle regulation, seed specificity, circadian rhythms, and fenestrated chloroplast differentiation (Figure 7).

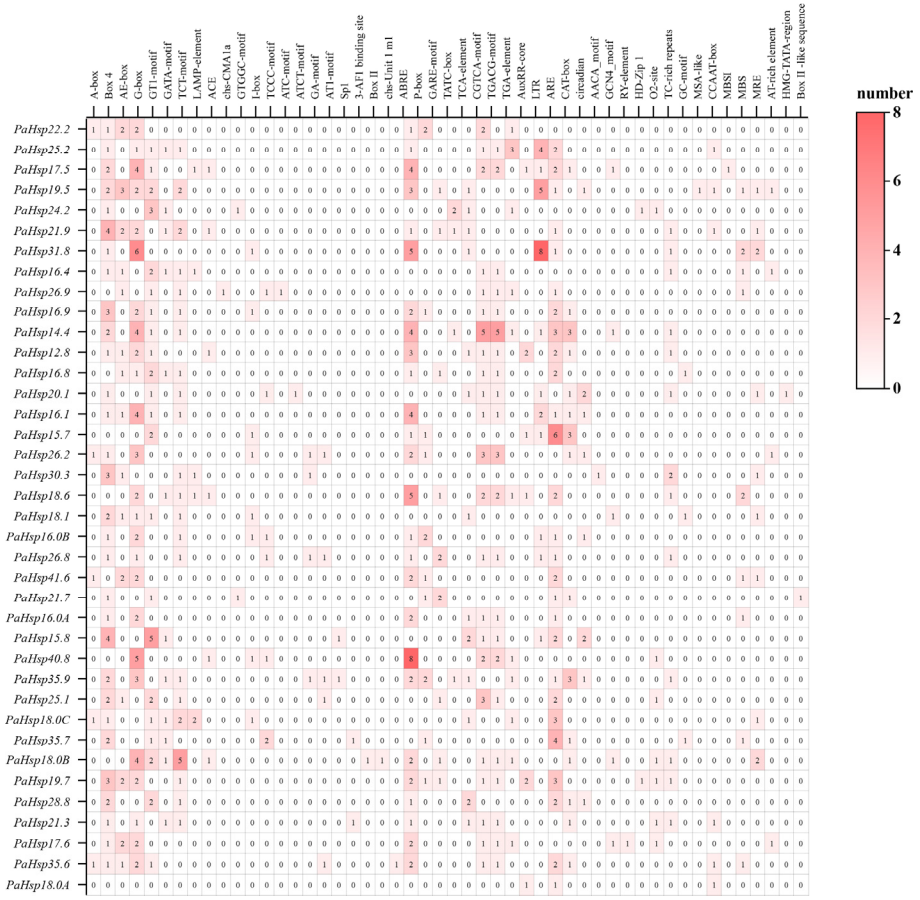


Figure 7. Number of cis-acting elements in the promoter of the *PaHsp20* gene family. The basic core sequences TATA-box and CAAT-box are not included in the figure; colors from white to red represent increasing numbers from 0 to 8.

Only *PaHsp30.3* had the AACA-motif element associated with endosperm-specific expression. Only *PaHsp17.6* had the cis-acting regulatory element associated with seed-specific regulation RY element. The cell cycle regulatory element MSA-like was present only in the *PaHsp19.5* gene. The MYB binding site involved in the regulation of flavonoid biosynthetic genes, the MBSI element, was present only in *PaHsp17.5* and it was speculated that these genes have unique regulatory capabilities.

3.5. The Expression Analysis of PhHsp20 Genes

We next confirmed the transcript level in specific tissues of the candidate *PhHsp* genes closely related to *PhMYC2a* using qRT-PCR analysis, which were obtained by RNA-Seq. The expression in petunia roots, stems, leaves, flowers, sepal, corolla, stamens, and pistils are shown in Figure 8. The expression of *PhHsp* was diverse but it was observed that

certain *Hsp* genes exhibited relatively high expression levels in specific tissues. For instance, *PhHsp16.1* had increased expression in flowers. *PhHsp40.8* showed significantly elevated expression in roots. In particular, *PhHsp21.9* and *PhHsp16.0A* demonstrated a prominent expression pattern. Additionally, *PhHsp16.8* had a high expression in several tissues.

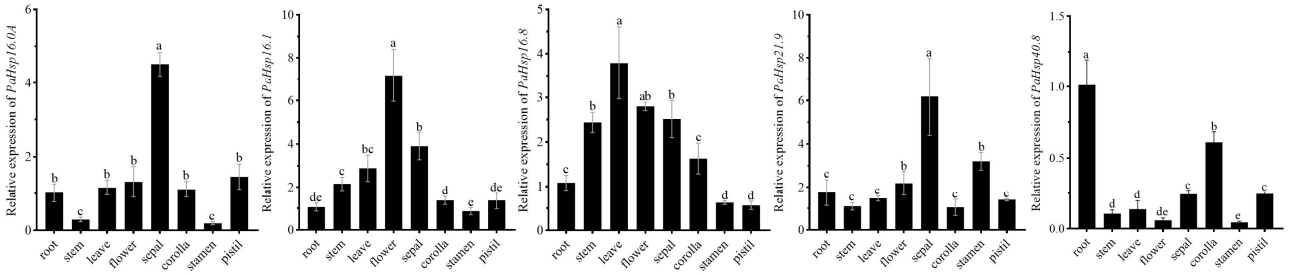


Figure 8. The expression patterns of *PhHsp20* genes in different petunia tissues. The RNA samples of roots, stems, leaves, flowers, sepal, corolla, stamens, and pistils were extracted from *P. hybrida* 'Michelle'. The expression levels of *PhHsp20* genes were detected by the $2^{-\Delta\Delta Ct}$ method with petunia EF-1α gene as the internal control, and the expression in the root was defined as one. The data were calculated from three replications and presented as mean values ± standard error. Different lowercase letters indicate significant differences in Tukey multiple comparisons ($p < 0.05$).

Developmental stage expression patterns of *PhHsp* genes during the growing processes of flower buds and anthers have been demonstrated represented by different length flower buds. The results of flower buds are shown in Figure 9A. *PhHsp40.8*, *PhHsp16.1*, and *PhHsp16.0A* genes had extremely high expression levels at periods of 0.2b, 2.5b, and 2.5b, respectively. However, they were relatively low at other periods, implying that these *PhHsp* genes might play important roles in such periods. On the contrary, *PhHsp16.8* and *PhHsp21.9* gene expression levels were relatively average in each period, suggesting that these genes might play a significant and continuous role during the bud development.

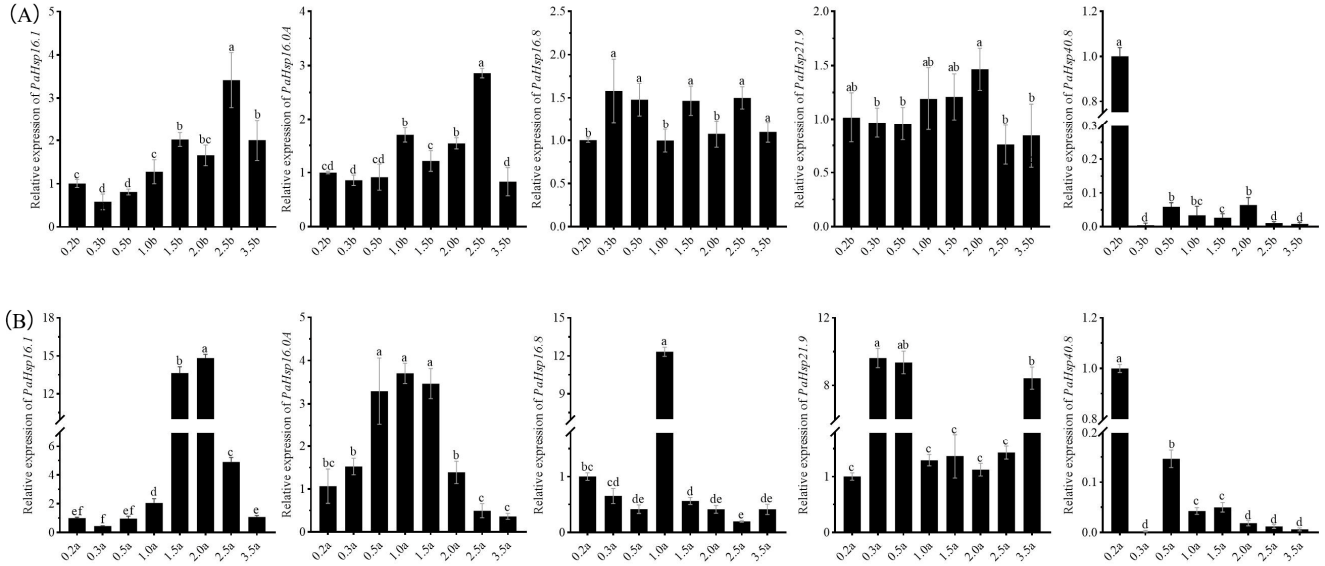


Figure 9. The expression analysis of *PhHsp20* genes during the development of petunia flower buds (**A**) and anthers (**B**). The RNA samples isolated from flower buds and anthers at seven developmental stages in *P. hybrida* 'Michelle'. The expression levels of *PhHsp20* genes were detected by the $2^{-\Delta\Delta Ct}$ method with petunia EF-1α gene as the internal control, and the expression in 0.2a stage was defined as one. The data were calculated from three replications and presented as mean values ± standard error. Different lowercase letters indicate significant differences in Tukey multiple comparisons ($p < 0.05$).

The expression of *PhHsp* genes in anthers fluctuated more compared to that in flower buds; all genes had exceptionally high expression levels in specific periods (Figure 9B). *PhHsp16.8* and *PhHsp40.8* genes had high expression levels at periods of 1.0a and 0.2a, respectively. Moreover, the remaining genes had high expression levels at several periods. For example, *PhHsp21.9* had high expression levels at periods of 0.3a, 0.5a, and 3.5a; *PhHsp16.1* (1.5a, 2.0a); *PhHsp16.0A* (0.5a, 1.0a, and 1.5a), indicating that it might play a crucial role in these periods.

3.6. Silencing of PhHsp16.0A and PhHsp16.1 Significantly Reduced the Stamen Fertility

According to the gene family identification results, among the five *Hsp20s* screened from the transcriptome, *PhHsp16.1* and *PhHsp16.0A* both belong to the subfamily. Y1H and dual-luciferase assays confirmed their direct binding to PhMYC2a. Additionally, qRT-PCR analysis revealed significant expression of these two genes during pollen development, suggesting their potential roles in this process.

To investigate the roles of *PhHsp16.0A* and *PhHsp16.1* in petunia flower development, we performed VIGS (Figure S1). qRT-PCR analysis of petunia seedlings one month post-injection revealed that the transcript levels of *PhHsp16.0A* and *PhHsp16.1* were significantly lower in silenced plants compared to pTRV2 controls (CK; Figure 10A,B), confirming successful silencing of the target genes. For subsequent experiments, we selected transgenic lines 1, 9, and 13 for *PhHsp16.1*, and lines 6, 11, and 12 for *PhHsp16.0A*.

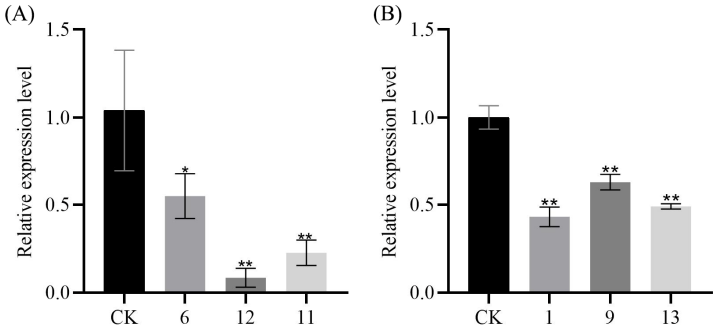


Figure 10. The qRT-PCR results of VIGS assay. (**A**) Expression levels in CK and pTRV2-*PhHsp16.0A* transgenic petunia plants; (**B**) expression levels in CK and pTRV2-*PhHsp16.1* transgenic petunia plants. The expression levels of *PhHsp* genes were detected by the $2^{-\Delta\Delta Ct}$ method with petunia EF-1α gene as the internal control. Asterisks represent statistically significant differences (* $p < 0.05$ and ** $p < 0.01$) as determined by Student's *t* test.

Following treatment with 1% aceto-carmine, wild-type pollen grains were mostly plump, spherical, and uniformly stained dark red (Figure 11A). In contrast, pollen grains from pTRV2-*PhHsp16.1* lines exhibited a significantly lower staining rate (Figure 11B). Additionally, the initiation and growth of pollen tubes in pTRV2-*PhHsp16.0A* lines were significantly reduced compared to those in fully viable pollen grains. Meanwhile, the observation results of other floral organs showed no significant difference compared with CK (Figures S2 and S3). These evidences suggested that the *Hsp20* gene played a critical role in stamen development.

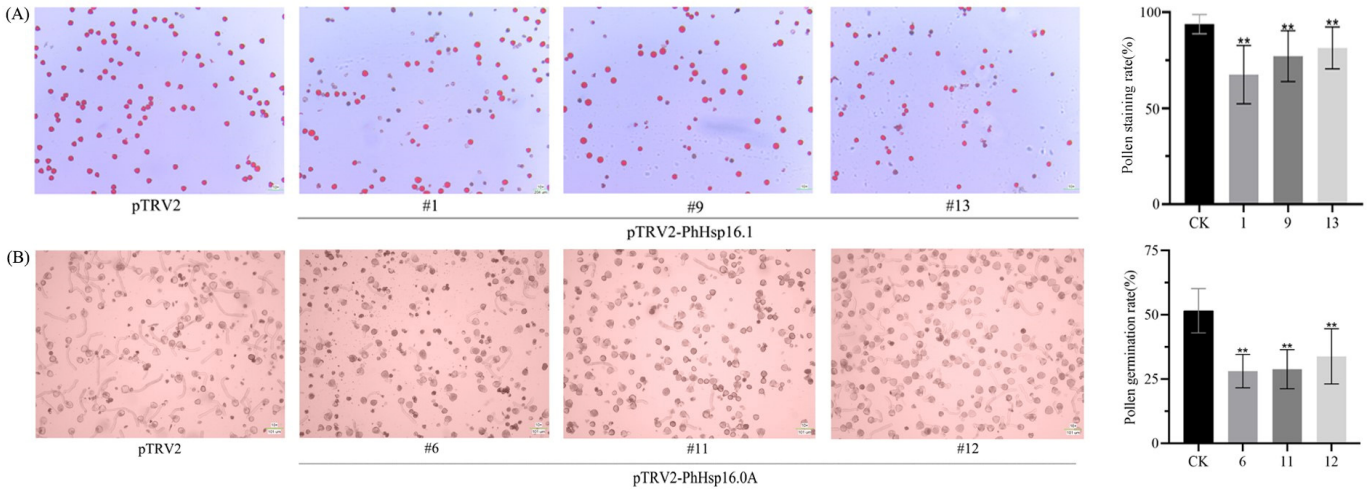


Figure 11. The result of pollen fertility test assay. (**A**) Pollen examination conducted by germination test from CK and line 1, 9, 13 of pTRV2-*PhHsp16.1* transgenic petunia plants; (**B**) Pollen examination conducted by staining test from CK and line 6, 11, 12 of pTRV2-*PhHsp16.0A* transgenic petunia plants; Asterisks represent statistically significant differences (** $p < 0.01$) as determined by Student's *t* test.

4. Discussion

Heat stress severely affects plant growth, causing physiological damage, physiological disorders, and biochemical alterations in plants at different stages of growth [35]. In recent years, the small heat shock protein gene family has been identified in numerous species. It has been reported that 63, 57, and 36 *Hsp20* family members were recently identified in *M. domestica*, *Populus yunnanensis*, and *Lactuca sativa*, respectively [24,36,37]. Numerous studies have demonstrated that small heat shock proteins are widespread in plants and play an important role in stress respond. Beyond stress conditions, *Hsp20* expression also undergoes significant changes during plant growth and development, with selective accumulation-specific organs such as seeds and pollen [38,39].

In this study, we used bioinformatics methods to mine and identify the *Hsp20* gene family of *P. axillaris* and obtained 38 *PaHsp20* gene family members. Phylogenetic analysis showed that 55.3% of the *PaHsp20* family genes were classified into the cytoplasmic C subclade, which was consistent with the taxonomic features of other species, like soybean [40], tomato [18], and apple [41], which all had the most cytoplasmic C subclade genes. Whereas differences in evolutionary analyses may be related to differences in the way of delineation. The CI subfamily of PaHsp20 represented the largest Hsp20 subfamily, consistent with findings in potato, Arabidopsis, and grape [15,23,42]. Comparative analysis of the *Hsp20* gene family between *P. axillaris* and its relative tomato revealed that tomato *Hsp20* genes are also classified into 13 subfamilies. Tomato, pepper, and petunia all lack the CVIII subfamily, while tomato and pepper both lack the CIV and MII subfamilies [17,18]. These findings suggest widespread occurrence of gene gain and loss events in plant evolution. Within the same plant family, certain subfamilies may be consistently absent across species, while others exhibit lineage-specific losses, reflecting divergent evolutionary trajectories.

Most of the proteins of this family are acidic proteins, which are the same as those of Hsp20 proteins of altospermum in the protologue community [43]. The *PaHsp20* genes show dispersed genomic distribution, with 38 family members distributed across 34 scaffolds. Three CI-subfamily genes (PaHsp18.0A, PaHsp18.0C, PaHsp35.7) co-localized on one scaffold, while two CII-subfamily genes (PaHsp31.8, PaHsp16.4) shared another scaffold. Notably, PaHsp20.1 (CII) and PaHsp16.1 (CI) co-occurred despite belonging to different subfamilies. UTR regions were rare among *PaHsp20* genes. Only six members contained 5′UTRs (*PaHsp16.8*, *PaHsp41.6*, *PaHsp30.3*, *PaHsp16.0B*, *PaHsp20.1*, *PaHsp21.3*), which may

regulate developmental processes including cell growth and tissue differentiation. Also, our results further revealed that the majority of *PaHsp20* genes (89.5%) contain no intron or only a single short intron. This structural feature aligns closely with observations in other plant species: 93.8% in grape, 97.14% in pepper, and 83.33% in tomato [17,18,23]. The consistency across these diverse species suggests that the fewer and shorter introns in *Hsp20* genes may represent a conserved evolutionary trait. Such a structural characteristic could confer functional advantages, as genes with fewer or shorter introns often undergo more rapid transcription and translation, which is particularly critical for Hsp20s given their role in rapid stress responses.

Given the diverse cis-acting elements in their promoter regions, these *PaHsp20* genes are likely involved in a wide range of biological processes and environmental responses. Most notably, the majority of *PaHsp20* members contain at least one light-responsive element and one phytohormone-related response element. This finding is supported in multiple species such as pepper and chickpeas [17,43]. This conservation of cis-acting element profiles across species suggests that the integration of light and phytohormone signals may represent a core regulatory mechanism for *Hsp20* genes in plants. In petunia, such elements could enable *PaHsp20* genes to fine-tune their expression in response to fluctuating light conditions (e.g., during floral development) and hormonal cues (such as those governing pollen maturation), thereby contributing to the coordination of growth and developmental processes. Thus, these elements likely position *PaHsp20* genes as key mediators of petunia growth and development, integrating both hormonal and environmental signals.

The previous research showed that *Hsp70* genes are required for normal plant development, including chloroplast development [44] and gametogenesis [45]. *Hsp70-16* dysfunction perturbs the proper development and function of floral organs, and loss of *Hsp17-16* function was found to cause the interruption of the lateral sepal opening, which would impair the normal development of floral organs in the subsequent pollination process [46]. Although Hsp70 and Hsp90, members of the heat shock protein superfamily, have been well-documented as playing critical roles in secondary metabolism and developmental regulation, the precise molecular mechanisms underlying the involvement of Hsp20 family proteins in these biological processes remain poorly characterized and require further elucidation.

While the *Hsp20* gene family has been extensively characterized for its roles in environmental stress responses, with most functional studies focusing on this context, our findings shed light on an underappreciated aspect of their biological significance. For instance, *AtHsp21* interacts with the pTAC5 protein and is important for chloroplast development in Arabidopsis under heat stress [47], and *CaHsp25.9* enhances tolerance to heat, salt, and drought by modulating reactive oxygen species accumulatio, antioxidant enzyme activity, and stress-related gene expression [48]. However, research exploring Hsp functions under non-stress conditions remains limited. Our work addresses this gap by identifying the gene family of *Hsp20* in petunia and establishing their direct regulation by the transcription factor PhMYC2a. This newly identified regulatory relationship extends the known functional repertoire of Hsp20 proteins, linking them to floral development in a non-stress context. By doing so, our study provides novel insights into the diverse roles of Hsp20s and offers a framework for investigating their understudied functions in plant developmental processes beyond stress responses.

Currently, the functional mechanisms of the MYC2 transcription factor in plants have been extensively characterized. As a key downstream effector in the JA pathway, MYC2 plays pivotal roles in regulating biotic and abiotic stress responses, plant growth and development, and the biosynthesis of specialized metabolites [49]. MYC2 exhibits diverse

DNA-binding specificities, including recognition of G-box (5′-CACGTG-3′) and E-box (5′-CACNTG-3′) motifs, and functions as both a transcriptional activator and repressor in modulating various aspects of JA signaling [50]. Numerous regulatory pathways involving MYC2 have been identified, such as MYC2-PUB22 [51], MYC2-EPF2/EPFL4/EPFL9 [52], and MYC2-GGPPS [53]. In the present study, we identified five PhHsp20 genes as direct downstream targets of PhMYC2a through Y1H and dual-luciferase assays. This finding provides the first evidence for a direct regulatory link between MYC2 and the Hsp20 gene family in petunia, thereby laying a foundation for refining the molecular regulatory network underlying stamen development in petunia. Notably, we verified the functions of *PhHsp16.0A* and *PhHsp16.1* in anther development using VIGS. However, due to the limitations of the VIGS technique, the target genes only exhibited reduced expression levels in the treated plants, resulting in a mere decrease in stamen fertility without the induction of complete male sterility. In future studies, constructing CRISPR/Cas9 vectors for *PhHsp16.0A* and *PhHsp16.1* to achieve targeted knockout of these genes will help clarify their precise regulatory capacity on stamen fertility, which will further advance our understanding of the MYC2-Hsp20 module in petunia reproductive development.

5. Conclusions

This study firstly mined five *Hsp20* genes downstream of PhMYC2a and validated their direct interaction using Y1H and dual-luciferase assays from the petunia transcriptome data. Secondly, we systematically classified and characterized the *Hsp20* gene family in the polyploid model species *P. axillaris*. The classification of PaHsp20 was based on phylogenetic analysis, conserved domain analysis, and gene structure analysis. Furthermore, the detailed analyses, including cis-element prediction, protein–protein interaction prediction, and tissue-specific expression analysis, suggest that some PaHsp20s might be involved in the regulation of plant growth. Finally, we validated the function of *PhHsp16.0A* and *PhHsp16.1* in reducing pollen fertility using virus-induced gene silencing (VIGS). This provides a possible direction for future studies on Hsp20 genes. This finding may offer a new avenue for future petunia breeding efforts.

Supplementary Materials: The following supporting information can be downloaded at: https://www.mdpi.com/article/10.3390/agronomy15092048/s1, Figure S1: The plants of VIGS assay (A) Representative images of wild-type (WT), control (CK), and VIGS-*PhHsp16.0A* transgenic petunia plants; (B) Representative images of WT, CK, and VIGS-*PhHsp16.1* transgenic petunia plants; Figure S2: Phenotypic observation results of *PhHsp16.1*; Figure S3: Phenotypic observation results of *PhHsp16.0A*; Table S1: Primers used in this research; Table S2: Locus ID information of Hsp20 used as query sequences in BLASTP analysis; Table S3: Naming of RNA-Seq samples; Table S4: The identification of PaHsp20 gene family members.

Author Contributions: X.Z.: writing—original draft, conceptualization, methodology, validation, formal analysis; B.Z. (Bingru Zhang): writing—original draft, visualization, software, methodology, formal analysis; Y.W.: methodology; L.W.: methodology; J.T.: methodology; B.Z. (Bingyan Zhao): methodology; Q.C.: methodology; J.G.: methodology; H.Z.: formal analysis; H.H.: writing—review and editing, supervision, project administration. All authors have read and agreed to the published version of the manuscript.

Funding: This research was funded by the National Natural Science Foundation of China (Grant No. 31972988), the Fundamental Research Funds for the Central Universities (Program No. BC2024103), and Hubei Provincial Innovation and Entrepreneurship Training Program for Undergraduate (No. S202410504120).

Data Availability Statement: The transcriptome data have been deposited in NCBI Sequence Read Archive (SRA, http://www.ncbi.nlm.nih.gov/Traces/sra accessed on 15 July 2025) with accession number PRJNA1308536.

Conflicts of Interest: The authors declare that they have no known competing financial interests or personal relationships that could have appeared to influence the work reported in this paper.

References

1. Zhang, H.Y.; Zhang, X.Y.; Ning, K.; Yan, X.L.; Wang, Q.J.; Huang, Z.X.; Zhu, Q.Q.; Zhao, L.; Zhang, Y.Q.; Ren, Y.; et al. Stamen and pollen development in Menispermaceae with contrasting androecium structure. *Plant Syst. Evol.* **2022**, *308*, 36. [CrossRef]
2. Song, S.S.; Qi, T.C.; Huang, H.; Xie, D.X. Regulation of Stamen Development by Coordinated Actions of Jasmonate, Auxin, and Gibberellin in Arabidopsis. *Mol. Plant* **2013**, *6*, 1065–1073. [CrossRef]
3. Fang, Y.X.; Guo, D.S.; Wang, Y.; Wang, N.; Fang, X.W.; Zhang, Y.H.; Li, X.; Chen, L.T.; Yu, D.Q.; Zhang, B.L.; et al. Rice transcriptional repressor OsTIE1 controls anther dehiscence and male sterility by regulating JA biosynthesis. *Plant Cell* **2024**, *36*, 1697–1717. [CrossRef]
4. Sachdev, S.; Biswas, R.; Roy, A.; Nandi, A.; Roy, V.; Basu, S.; Chaudhuri, S. The Arabidopsis ARID–HMG DNA-BINDING PROTEIN 15 modulates jasmonic acid signaling by regulating MYC2 during pollen development. *Plant Physiol.* **2024**, *196*, 996–1013. [CrossRef]
5. Yu, J.P.; Wu, Z.; Liu, X.Y.; Fang, Q.Q.; Pan, X.; Xu, S.J.; He, M.; Lin, J.X.; Teng, N.J. LoBLH6 interacts with LoMYB65 to regulate anther development through feedback regulation of gibberellin synthesis in lily. *Hortic. Res.* **2025**, *12*, uhae339. [CrossRef]
6. Song, S.Y.; Chen, Y.; Liu, L.; See, Y.H.B.; Mao, C.Z.; Gan, Y.B.; Yu, H. OsFTIP7 determines auxin-mediated anther dehiscence in rice. *Nat. Plants* **2018**, *4*, 495–504. [CrossRef]
7. Chen, S.F.; Lou, S.L.; Zhao, X.C.; Zhang, S.J.; Chen, L.T.; Huang, P.; Li, G.D.; Li, Y.Y.; Liu, Y.G.; Chen, Y.L. Ectopic expression of a male fertility gene, LOGL8, represses LOG and hinders panicle and ovule development. *Crop J.* **2022**, *10*, 1665–1673. [CrossRef]
8. Zhang, Q.Q.; Wang, X.; Zhao, T.Y.; Luo, J.F.; Liu, X.; Jiang, J. CYTOSOLIC INVERTASE2 regulates flowering and reactive oxygen species-triggered programmed cell death in tomato. *Plant Physiol.* **2024**, *196*, 1110–1125. [CrossRef]
9. Li, P.; Tian, J.; Guo, C.; Luo, S.; Li, J. Interaction of gibberellin and other hormones in almond anthers: Phenotypic and physiological changes and transcriptomic reprogramming. *Hortic. Res.* **2021**, *8*, 94. [CrossRef]
10. UI Haq, S.; Khan, A.; Ali, M.; Khattak, A.M.; Gai, W.X.; Zhang, H.X.; Wei, A.M.; Gong, Z.H. Heat shock proteins: Dynamic biomolecules to counter plant biotic and abiotic stresses. *Int. J. Mol. Sci.* **2019**, *20*, 5321. [CrossRef]
11. Hartl, F.U.; Bracher, A.; Hayer-Hartl, M. Molecular chaperones in protein folding and proteostasis. *Nature* **2011**, *475*, 324–332. [CrossRef]
12. Balchin, D.; Hayer-Hartl, M.; Hartl, F.U. In vivo aspects of protein folding and quality control. *Science* **2016**, *353*, acc4353. [CrossRef]
13. Wang, W.; Vinocur, B.; Shoseyov, O.; Altman, A. Role of plant heat-shock proteins and molecular chaperones in the abiotic stress response. *Trends Plant Sci.* **2004**, *9*, 244–252. [CrossRef]
14. Waters, E.R. The evolution, function, structure, and expression of the plant *sHSPs*. *J. Exp. Bot.* **2013**, *64*, 391–403. [CrossRef]
15. Siddique, M.; Gernhard, S.; von Koskull-Döring, P.; Vierling, E.; Scharf, K.-D. The plant *sHSP* superfamily: Five new members in *Arabidopsis thaliana* with unexpected properties. *Cell Stress Chaperon.* **2008**, *13*, 183–197. [CrossRef]
16. Sarkar, N.K.; Kim, Y.K.; Grover, A. Rice *sHsp* genes: Genomic organization and expression profiling under stress and development. *BMC Genom.* **2009**, *10*, 393. [CrossRef]
17. Guo, M.; Liu, J.H.; Lu, J.P.; Zhai, Y.F.; Wang, H.; Gong, Z.H.; Wang, S.B.; Lu, M.H. Genome-wide analysis of the *CaHsp20* gene family in pepper: Comprehensive sequence and expression profile analysis under heat stress. *Front. Plant Sci.* **2015**, *6*, 806. [CrossRef]
18. Yu, J.H.; Cheng, Y.; Feng, K.; Ruan, M.Y.; Ye, Q.J.; Wang, R.Q.; Li, Z.M.; Zhou, G.Z.; Yao, Z.P.; Yang, Y.J.; et al. Genome-wide identification and expression profiling of tomato *Hsp20* gene family in response to biotic and abiotic stresses. *Front. Plant Sci.* **2016**, *17*, 1215. [CrossRef]
19. Huang, J.J.; Hai, Z.X.; Wang, R.Y.; Yu, Y.Y.; Chen, X.; Liang, W.H.; Wang, H.H. Genome-wide analysis of *HSP20* gene family and expression patterns under heat stress in cucumber (*Cucumis sativus* L.). *Front. Plant Sci.* **2022**, *13*, 968418. [CrossRef]
20. Wang, C.; Wang, X.J.; Zhou, P.; Li, C.C. Genome-wide identification and characterization of *RdHSP* genes related to high temperature in *Rhododendron delavayi*. *Plants* **2024**, *13*, 1878. [CrossRef]
21. Dafny-Yelin, M.; Tzfira, T.; Vainstein, A.; Adam, Z. Non-redundant functions of sHSP-CIs in acquired thermotolerance and their role in early seed development in Arabidopsis. *Plant Mol. Biol.* **2008**, *67*, 363–373. [CrossRef]

22. Chauhan, H.; Khurana, N.; Nijhavan, A.; Khurana, J.P.; Khurana, P. The wheat chloroplastic small heat shock protein (sHSP26) is involved in seed maturation and germination and imparts tolerance to heat stress. *Plant Cell Environ.* **2012**, *35*, 1912–1931. [CrossRef]
23. Ji, X.R.; Yu, Y.H.; Ni, P.Y.; Zhang, G.H.; Guo, D.L. Genome-wide identification of small heat-shock protein (*HSP20*) gene family in grape and expression profile during berry development. *BMC Plant Biol.* **2019**, *19*, 433. [CrossRef]
24. Zhang, F.J.; Li, Z.Y.; Zhang, D.E.; Ma, N.; Wang, Y.X.; Zhang, T.T.; Zhao, Q.; Zhang, Z.; You, C.X.; Lu, X.Y. Identification of *Hsp20* gene family in *Malus* domestica and functional characterization of *Hsp20* class I gene *MdHsp18.2b*. *Physiol. Plant.* **2024**, *176*, e14288. [CrossRef]
25. Lian, X.D.; Wang, Q.P.; Li, T.H.; Gao, H.Z.; Li, H.N.; Zheng, X.B.; Feng, J.C. Phylogenetic and transcriptional analyses of the *HSP20* gene family in peach revealed that *PpHSP20-32* is involved in plant height and heat tolerance. *Int. J. Mol. Sci.* **2022**, *23*, 10849. [CrossRef]
26. Vandenbussche, M.; Chambrier, P.; Rodrigues Bento, S.; Morel, P. Petunia, your next supermodel? *Front. Plant Sci.* **2016**, *7*, 72. [CrossRef]
27. Smith, A.G.; Gardner, N.; Zimmermann, E. Increased flower longevity in petunia with male sterility. *Hortscience* **2004**, *39*, 822. [CrossRef]
28. García-Sogo, B.; Pineda, B.; Roque, E.; AntÓn, T.; Atarés, A.; Borja, M.; Beltrán, J.P.; Moreno, V.; Cañas, L.A. Production of engineered long-life and male sterile Pelargonium plants. *BMC Plant Biol.* **2012**, *12*, 156–171. [CrossRef]
29. Li, S.R.; Hu, Y.; Yang, H.Q.; Tian, S.B.; Wei, D.Y.; Tang, Q.L.; Yang, Y.; Wang, Z.M. The regulatory roles of MYC TFs in plant stamen development. *Plant Sci.* **2023**, *333*, 111734. [CrossRef]
30. Xie, J.M.; Chen, Y.R.; Cai, G.J.; Cai, R.L.; Hu, Z.; Wang, H. Tree Visualization by One Table (tvBOT): A web application for visualizing, modifying and annotating phylogenetic trees. *Nucleic Acids Res.* **2023**, *51*, W587–W592. [CrossRef]
31. Lescot, M.; Déhais, P.; Thijs, G.; Marchal, K.; Moreau, Y.; Van de Peer, Y.; Rouzé, P.; Rombauts, S. PlantCARE, a database of plant cis-acting regulatory elements and a portal to tools for in silico analysis of promoter sequences. *Nucleic Acids Res.* **2002**, *30*, 325–327. [CrossRef]
32. Li, T.; Jiang, Z.; Zhang, L.; Tan, D.; Wei, Y.; Yuan, H.; Li, T.; Wang, A. Apple (*Malus domestica*) MdERF2 negatively affects ethylene biosynthesis during fruit ripening by suppressing *MdACS1* transcription. *Plant J.* **2016**, *88*, 735–748. [CrossRef] [PubMed]
33. Yue, Y.Z.; Zhu, W.W.; Wang, J.H.; Wang, T.T.; Shi, L.S.; Thomas, H.R.; Hu, H.R.; Wang, L.G. Integration of DNA methylation, microRNAome, degradome and transcriptome provides insights into petunia anther development. *Plant Cell Physiol.* **2024**, *66*, 36–49. [CrossRef]
34. Huang, X.; Yue, Y.Z.; Sun, J.; Peng, H.; Yang, Z.N.; Bao, M.Z.; Hu, H.R. Characterization of a fertility-related SANT/MYB gene (*PhRL*) from petunia. *Sci. Hortic.* **2015**, *183*, 152–159. [CrossRef]
35. Hassan, M.U.; Chattha, M.U.; Khan, I.; Chattha, M.B.; Barbanti, L.; Aamer, M.; Iqbal, M.M.; Nawaz, M.; Mahmood, A.; Ali, A.; et al. Heat stress in cultivated plants: Nature, impact, mechanisms, and mitigation strategies—A review. *Plant Biosyst.* **2021**, *155*, 211–234. [CrossRef]
36. Shi, L.C.; Kang, Y.D.; Ding, L.; Xu, L.J.; Liu, X.J.; Yu, A.M.; Liu, A.Z.; Li, P. Comprehensive characterization of poplar *HSP20* gene family: Genome-wide identification, stress-induced expression profiling, and protein interaction verifications. *BMC Plant Biol.* **2025**, *25*, 251. [CrossRef]
37. Zhang, Q.Q.; Dai, B.W.; Fan, M.; Yang, L.L.; Li, C.; Hou, G.G.; Wang, X.F.; Gao, H.B.; Li, J.R. Genome-wide profile analysis of the Hsp20 family in lettuce and identification of its response to drought stress. *Front. Plant Sci.* **2024**, *15*, 1426719. [CrossRef]
38. Ham, D.J.; Moon, J.C.; Hwang, S.G.; Jang, C.S. Molecular characterization of two small heat shock protein genes in rice: Their expression patterns, localizations, networks, and heterogeneous overexpressions. *Mol. Biol. Rep.* **2013**, *40*, 6709–6720. [CrossRef]
39. Roger, D.K.; Tamutenda, C.; Hannah, S.T.; Tea, M.; Robert, A.B.; Virginia, B.P. Chaperone function of two small heat shock proteins from maize. *Plant Sci.* **2014**, *221–222*, 48–58. [CrossRef]
40. Lopes-Caitar, V.S.; de Carvalho, M.C.; Darben, L.M.; Kuwahara, M.K.; Nepomuceno, A.L.; Dias, W.P.; Abdelnoor, R.V.; Marcelino-Guimarães, F.C. Genome-wide analysis of the *Hsp20* gene family in soybean: Comprehensive sequence, genomic organization and expression profile analysis under abiotic and biotic stresses. *BMC Genom.* **2013**, *28*, 577.
41. Yao, F.W.; Song, C.H.; Wang, H.T.; Song, S.W.; Jiao, J.; Wang, M.M.; Zheng, X.B.; Bai, T.H. Genome-wide characterization of the *HSP20* gene family identifies potential members involved in temperature stress response in apple. *Front. Genet.* **2020**, *11*, 609184. [CrossRef]
42. Li, Y.L.; Li, Z.M.; Dong, L.P.; Tang, M.; Zhang, P.; Zhang, C.H.; Cao, Z.Y.; Zhu, Q.; Chen, Y.C.; Wang, H.; et al. Histone H1 acetylation at lysine 85 regulates chromatin condensation and genome stability upon DNA damage. *Nucleic Acids Res.* **2018**, *46*, 7716–7730. [CrossRef]
43. Liu, S.S.; Wu, Y.Z.; Yang, L.; Zhang, Z.B.; He, D.D.; Yan, J.G.; Zou, H.S.; Liu, Y.M. Genome-wide identification and expression analysis of heat shock protein 20 (HSP20) gene family in response to high-temperature stress in chickpeas (*Cicer arietinum* L.). *Agronomy* **2024**, *14*, 1696. [CrossRef]

44. Latijnhouwers, M.; Xu, X.M.; Møller, S.G. Arabidopsis stromal 70-kDa heat shock proteins are essential for chloroplast development. *Planta* **2010**, *232*, 567–578. [CrossRef]
45. Maruyama, D.; Sugiyama, T.; Endo, T.; Nishikawa, S. Multiple *BiP* genes of *Arabidopsis thaliana* are required for male gametogenesis and pollen competitiveness. *Plant Cell Physiol.* **2014**, *55*, 801–810. [CrossRef]
46. Chen, X.; Shi, L.; Chen, Y.Q.; Zhu, L.; Zhang, D.S.; Xiao, S.; Aharoni, A.; Shi, J.X.; Xu, J. Arabidopsis HSP70-16 is required for flower opening under normal or mild heat stress temperatures. *Plant Cell Environ.* **2019**, *42*, 1190–1204. [CrossRef]
47. Zhong, L.L.; Zhou, W.; Wang, H.J.; Ding, S.H.; Lu, Q.T.; Wen, X.G.; Peng, L.W.; Zhang, L.X.; Lu, C.M. Chloroplast small heat shock protein HSP21 interacts with plastid nucleoid protein pTAC5 and is essential for chloroplast development in *Arabidopsis* under heat stress. *Plant Cell* **2013**, *25*, 2925–2943. [CrossRef]
48. Feng, X.H.; Zhang, H.X.; Ali, M.; Gai, W.X.; Cheng, G.X.; Yu, Q.H.; Yang, S.B.; Li, X.X.; Gong, Z.H. A small heat shock protein *CaHsp25.9* positively regulates heat, salt, and drought stress tolerance in pepper (*Capsicum annuum* L.). *Plant Physiol. Biochem.* **2019**, *142*, 151–162. [CrossRef]
49. Luo, L.; Wang, Y.; Qiu, L.; Han, X.; Zhu, Y.; Liu, L.; Man, M.; Li, F.; Ren, M.; Xing, Y. MYC2: A Master Switch for Plant Physiological Processes and Specialized Metabolite Synthesis. *Int. J. Mol. Sci.* **2023**, *24*, 3511. [CrossRef]
50. Kazan, K.; Manners, J.M. MYC2: The Master in Action. *Mol. Plant* **2013**, *6*, 686–703. [CrossRef]
51. Wu, S.F.; Hu, C.Y.; Zhu, C.G.; Fan, Y.F.; Zhou, J.; Xia, X.J.; Shi, K.; Zhou, Y.H.; Foyer, H.C.; Yu, J.Q. The MYC2–PUB22–JAZ4 module plays a crucial role in jasmonate signaling in tomato. *Mol. Plant* **2024**, *17*, 598–613. [CrossRef] [PubMed]
52. Xia, Y.; Jiang, S.; Wu, W.; Du, K.; Kang, X. MYC2 regulates stomatal density and water use efficiency via targeting EPF2/EPFL4/EPFL9 in poplar. *New Phytol.* **2024**, *241*, 2506–2522. [CrossRef]
53. Zheng, J.R.; Liao, Y.L.; Ye, J.B.; Xu, F.; Zhang, W.W.; Zhou, X.; Wang, L.N.; He, X.; Cao, Z.Y.; Yi, Y.W.; et al. The transcription factor MYC2 positively regulates terpene trilactone biosynthesis through activating *GbGGPPS* expression in *Ginkgo biloba*. *Hortic. Res.* **2024**, *11*, uhae228. [CrossRef]

Disclaimer/Publisher's Note: The statements, opinions and data contained in all publications are solely those of the individual author(s) and contributor(s) and not of MDPI and/or the editor(s). MDPI and/or the editor(s) disclaim responsibility for any injury to people or property resulting from any ideas, methods, instructions or products referred to in the content.